UDC 538.935 doi: 10.15407/hftp08.01.018

L.A. Karachevtseva [1, 2], M.T. Kartel [1, 3], K.P. Konin [2], O.O. Lytvynenko [2], V.F. Onyshchenko [2], Wang Bo [1]

LIGHT EMITTING "POLYMER-NANOPARTICLES" COATINGS ON MACROPOROUS SILICON SUBSTRATES

[1] Ningbo University of Technology, No.55-155 Cui Bai Road, Ningbo 315016, China
[2] V.Lashkaryov Institute of Semiconductor Physics of National Academy of Sciences of Ukraine 41 Nauki Ave., Kyiv, 03028, Ukraine, E-mail: lakar@isp.kiev.ua
[3] Chuiko Institute of Surface Chemistry of National Academy of Sciences of Ukraine 17 General Naumov Str., Kyiv, 03164, Ukraine

We investigate the conditions for increase of the photoluminescence of CdS nanocrystals in polyethyleneimine and polyethyleneimine with carbon multiwall nanotubes on macroporous silicon substrates. Macroporous silicon structures are made using the photoelectrochemical etching of n-Si wafers. Macropores with diameter $D_p = 2 \div 5$ μm, depth $h_p = 40 \div 120$ μm and concentration $N_p = (1 \div 6) \cdot 10^6$ cm^{-2} were formed. CdS nanocrystals of 1.8–2 nm in size are synthesized in reaction between Cd^{2+} and HS^- in a colloidal solution of polyethyleneimine in water. Carbon multiwall high purity nanotubes with submicron length and 20 nm diameter were produced by catalytic pyrolysis of unsaturated hydrocarbons. "Polymer-nanoparticles" coatings are deposited from a colloidal solution in water on single crystalline silicon, macroporous silicon and oxidized macroporous silicon. The maximal photoluminescence intensity of CdS nanocrystals is measured for the oxidized macroporous silicon substrates with maximal electric field strength at the Si-SiO_2 interface. The photoluminescence quantum yield of CdS nanocrystals on the surface of oxidized macroporous silicon increases with time and reaches 28 %. Photoluminescence of polyethyleneimine with carbon multiwall nanotubes on macroporous silicon with microporous layer is 3–6 times more intense as compared with substrates c-Si, macroporous Si and oxidized macroporous Si due to a non-radiative proton recombination decrease at the silicon matrix boundary with microporous layer and nanocoating.

Keywords: *macroporous silicon substrates, polyethyleneimine, CdS nanocrystals, multiwall carbon nanotubes*

INTRODUCTION

Currently considerable interest exists in the light-emitting semiconductor nanocrystals based on II-VI compounds. This is due to the successes achieved by colloid chemistry in the synthesis of such structures [1]. The researches in this area are focused on the development of nanocrystals in a dielectric matrix to reduce non-radiative recombination. The dependence of photoluminescence of CdSe nanoparticles and CdSe/ZnS on the matrix material (substrate) is studied on the base of organic semiconductors and quartz [2]. Nanostructures based on semiconductor materials have promising applications including the optoelectronic devices such as light-emitting diodes [3] and next generation of quantum dot solar cells [4]. Moreover, nanoscale semiconductors functionalized with biomolecules are promising as molecular fluorescent probes in biological applications [5]. Deposition of light-emitting nanocrystals on structured silicon substrates will favor development of new waveguide amplifiers and lasers for silicon micro- and nanophotonics. The size-selective photoetching technique and the dependence of photoluminescence (PL) of nanoparticles on the matrix material were developed and studied [6, 7]. The development of methods for obtaining well-defined polymer–QD hybrid materials with tunable optical properties is an active field of research [8]. Narrow-band luminescence has been

observed at the short-wavelength edge of the luminescence spectrum of polyethylene and polytetrafluoroethylene. The characteristics of this luminescence permit its assignment to the radiation emitted in recombination of ruptured C-C bonds in polymer chains [9].

Macroporous silicon is a promising material for the development of 2D photonic structures with the required geometry and large effective surface [10, 11]. 2D macroporous silicon structures formed by photoelectrochemical etching on silicon substrates [10] are promising for photoelectrical [12], optical [13] and biosensors [14]. Light-emitting nanocrystals on macroporous silicon matrix are promising for the development of "white" light sources [1], completely inorganic multicolor LEDs [6]. Light-emitting coatings of CdS nanocrystals on macroporous silicon substrates are light concenters [3] for silicon solar cells. This is due to photoluminescence excitation in the visible spectral range after illumination by UV light. This effect is useful to increase the spectral range of light absorption by solar cells [4] because of conversion of UV radiation into visible light. Local electric fields at the "macropore-nanocoating" interface [15] increase the resulted electron flow from the silicon matrix toward the nanocrystal layer and reduce the non-radiative recombination in light-emitting nanocoatings. The strength of a local electric field can be determined from the Wannier–Stark effect [16].

In this paper, light-emitting coatings of CdS nanocrystals in polyethyleneimine (PEI) [1] and polyethyleneimine with multiwall carbon nanotubes [17] on silicon substrates are investigated. The conditions for increase in the CdS nanocrystal photoluminescence of the oxidized macroporous silicon structures due to surface local electric fields and the counter flow of electrons from the silicon matrix toward the CdS nanocrystal layer are evaluated. The structures with nanocoatings of polyethyleneimine with multiwall carbon nanotubes on macroporous silicon with microporous silicon layers have been proposed for fabrication of efficient light-emitting elements due to decrease of the non-radiative recombination at the silicon-nanocoating interface.

EXPERIMENT

Macroporous silicon structures with arbitrary distribution of macropores were made of silicon wafers characterized by the [100] orientation and *n*-type of conductivity (the electron concentration $n_0 = 10^{15}$ cm^{-3}). We used the technique of electrochemical etching at illumination of the backside of a silicon substrate (thickness $H = 520$ μm) [18, 19].

The initial samples are combined micropore-macropore silicon structures consisting of 100 nm micropore layers on macropore walls. Addition anisotropic etching in 10 % solution of KOH removes the microporous layers from macropore walls. A fragment of the macroporous silicon structure with arbitrary distribution of macropores and the macropore profile are presented in Fig. 1 *a*. According to the results of optical microscopy, macropores with diameter $D_p = 2 \div 5$ μm and concentration $N_p = (1 \div 6) \cdot 10^6$ cm^{-2} were formed. The macropore depth was $h_p = 40 \div 120$ μm. Fig. 2 *b* shows a fragment of the oxidized macroporous silicon structure and direction of light incidence on the sample with SiO_2 nanocoatings and CdS nanocrystals in PEI.

CdS nanocrystals 1.8-2 nm in size (Fig. 2 *a*) were synthesized in reaction between Cd^{2+} and HS^- in a colloidal solution of polyethyleneimine in water [1]. The samples obtained were washed with distilled water to remove external salts. Fig. 2 *a* shows morphology of CdS nanocrystals in polyethyleneimine according to the atomic force microscopy (AFM) data, which confirmed that the sizes of CdS nanocrystals are about 2 nm. Coatings of CdS nanocrystals in polyethyleneimine were deposited from a colloidal solution in water on (1) single crystalline silicon, (2) macroporous silicon and (3) oxidized macroporous silicon (Fig. 1 *b*).

Carbon multiwall high purity nanotubes with submicron length and 20 nm diameter (Fig. 2 *b*) were produced by catalytic pyrolysis of unsaturated hydrocarbons (propylene C_3H_6) [20]. Carbon multiwall nanotubes were deposited from a colloidal solution of polyethyleneimine in water onto (1) single crystalline silicon, (2) macroporous silicon, (3) oxidized macroporous silicon, and (4) macroporous silicon with microporous silicon layer.

The macroporous surface cleaning was provided by preliminary oxidation in atmosphere of dry oxygen at 900 °C for 15 min (the oxide thickness of 30 nm) and further oxide etching off in 10 % aqueous solution of HF.

Such a procedure reduces the concentration of non-radiative recombination centers (mainly hydrogen). SiO_2 nanocoatings were formed in the diffusion stove after treatment in the nitrogen atmosphere. The oxide layers (thickness of 5÷200 nm) were formed on macroporous silicon samples by exposure in dry oxygen for 40÷60 min at the temperature of 1050 °C. The oxide thickness was measured using ellipsometry with 0.2 nm accuracy.

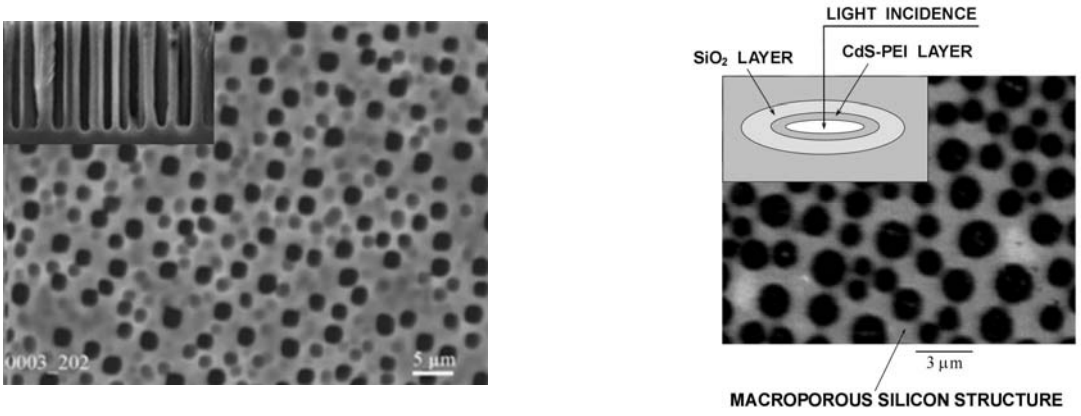

a *b*

Fig. 1. *a* – A fragment of the macroporous silicon structure with arbitrary distribution of macropores; insert: macropore profile; *b* – direction of light incidence along the main axis of cylindrical macropores on the sample with SiO_2 nanocoatings and CdS nanocrystals in PEI

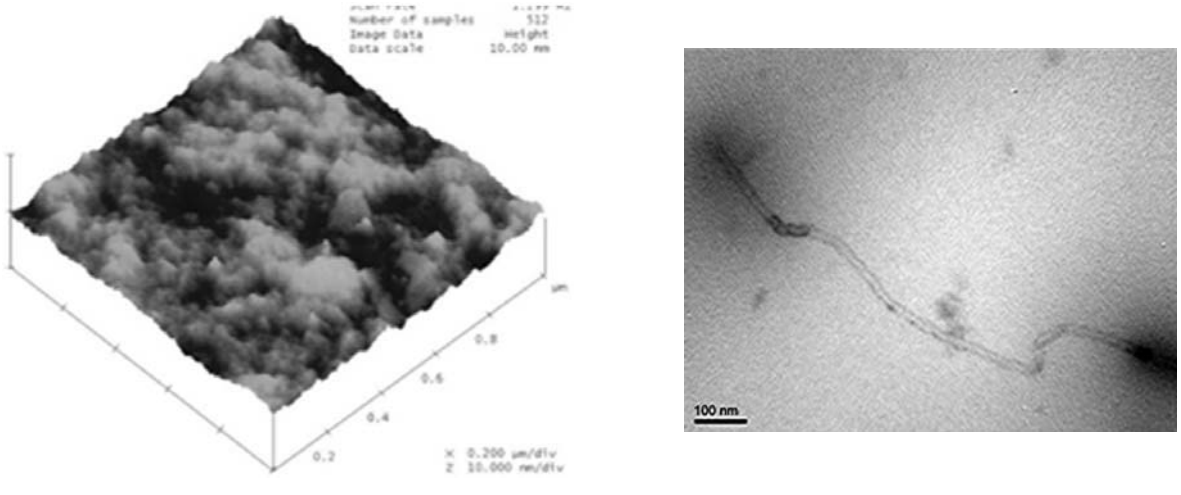

a *b*

Fig. 2. *a* – Morphology of CdS nanocrystals in PEI according to the AFM data, *b* – microphotograph of the typical carbon multiwall nanotube with more than one micron length and about 20 nm diameter

Nanoparticle morphology (Fig. 2 *a*) was investigated by AFM (a NanoScope IIIa Dimension 3000^{TM}). The chemical states on the surface of macroporous silicon structures with nanocoatings and the electric field at the Si-SiO_2 boundary were identified by IR absorption spectra using a Perkin Elmer Spectrum BXII IR Fourier spectrometer in the spectral range of 300÷8000 cm^{-1}. The optical absorption spectra were measured at normal incidence of IR radiation on the sample (Fig. 1 *b*). The spectral measurement error was about 2 cm^{-1}. Raman spectra of macroporous silicon structures with nanocoatings of polyethyleneimine with

multiwall carbon nanotubes were measured using a Horiba Jobin-Yvon T64000 spectrometer. The photoluminescence spectra of the nanocoatings on macroporous silicon samples were obtained in the 1.8–3.3 eV range of photon energy. The excitation radiation with photon energy of 0.34 eV falls on the sample through an optical fiber, and photoluminescence emission of the test sample falls on the sensor and the optical fiber through a slit with width of 2.5 nm. The angle between the excitation radiation and photoluminescence emission is 5º. IR absorption, Raman and photoluminescence spectra measurements were carried out in air at room temperature.

RESULTS

The IR absorption spectra of macroporous silicon structures before (*1*) and after (*2*) surface cleaning are shown in Fig. 3 *a*.

The IR absorption spectra of oxidized macroporous silicon structures after preliminary surface cleaning with next surface oxidation (oxide thickness of 5÷20 nm) as well as without surface cleaning and next surface oxidation (oxide thickness of 7÷30 nm) are shown in Fig. 3 *b*.

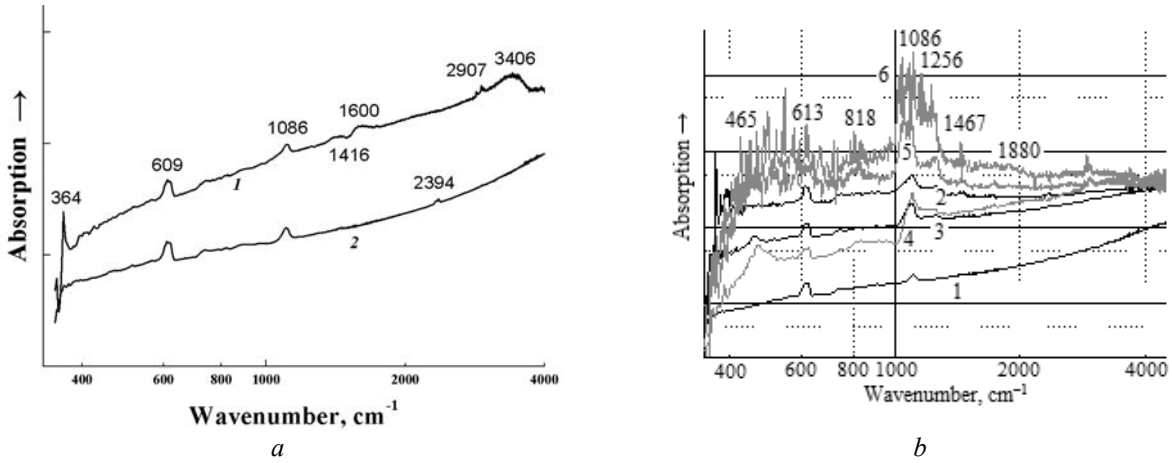

Fig. 3. *a* – IR absorption spectra of macroporous silicon structure before (*1*) and after (*2*) surface cleaning. *b* – IR absorption spectra of oxidized macroporous silicon structures after surface cleaning and oxidation; oxide thickness: *1* – 5 nm, *2* – 10 nm, *3* – 20 nm; IR absorption spectra of oxidized macroporous silicon structures without surface cleaning and with oxidation; oxide thickness: *4* – 7 nm, *5* – 15 nm and *6* – 30 nm

The IR absorption of macroporous silicon with surface oxide thickness of 5 nm is 1.5 times greater than that without surface oxidation. Both the nature and intensity of absorption peaks are almost identical. The IR spectrum of the macroporous silicon sample with surface oxide thickness of 10 nm changes dramatically. We measured a 364 cm^{-1} peak of one-phonon absorption and a 465 cm^{-1} peak associated with Si-O-Si rotation [14]. There is a strong growth of the Si-O-Si oxide peak (1095 cm^{-1}) for structures without surface cleaning and next surface oxidation (oxide thickness of 7÷30 nm). In addition to the TO phonon peaks (1086–1095 cm^{-1}), LO phonon absorption peaks (1250–1256 cm^{-1}) appear due to radiation incidence along the surface of cylindrical macropores (geometry of frustrated total internal reflection [21]). Additional absorption peaks appear in the spectral regions of TO and LO phonons. A series of light absorption bands at $\omega \geq \omega_{LO}$ can be explained by formation of multiphonon states $(\omega_S^+)_N = \omega_{TO}[N(\varepsilon_0/\varepsilon_\infty)^{1/2} - (N–1)]$ as a result of interaction of phonons of the SiO_2 film with waveguide modes in the silicon matrix. In our case, the guided and quasi-guided modes are formed on a silicon matrix, with parameters of modes equal to the distance between the macropores. As a result, absorption increases as the frequency $(\omega_S^+)_N$ of the *N*-th mode of surface phonon-polariton coincides with the frequencies of the waveguide modes.

Fig. 4 *a* shows a fragment the IR spectra of macroporous silicon after surface cleaning and oxidation to 10 nm thick oxide (*1*) and without surface cleaning and with oxidation to 15 nm thick oxide (*2*).

Absorption of macroporous silicon samples without oxidation and oxide removal exceeds about 10 times that of macroporous silicon samples with preliminary cleaning. The oscillations of IR absorption result from electron resonance scattering in a strong electric field by impurity states on the surface of macropores, with the difference between two resonance energies $\Delta E = Fa = 8 \div 10$ cm^{-1} equal to the Wannier–Stark step [16]. The oscillations have small amplitudes of IR absorption and nearly the same period for samples with surface cleaning and those of macroporous silicon without preliminary surface cleaning. A sharp decrease of the oscillation amplitude in the electro-optical effects is determined by an increase of the broadening parameter Γ [22] and relevant decrease of the electron scattering lifetime τ on Si-SiO_2 surface.

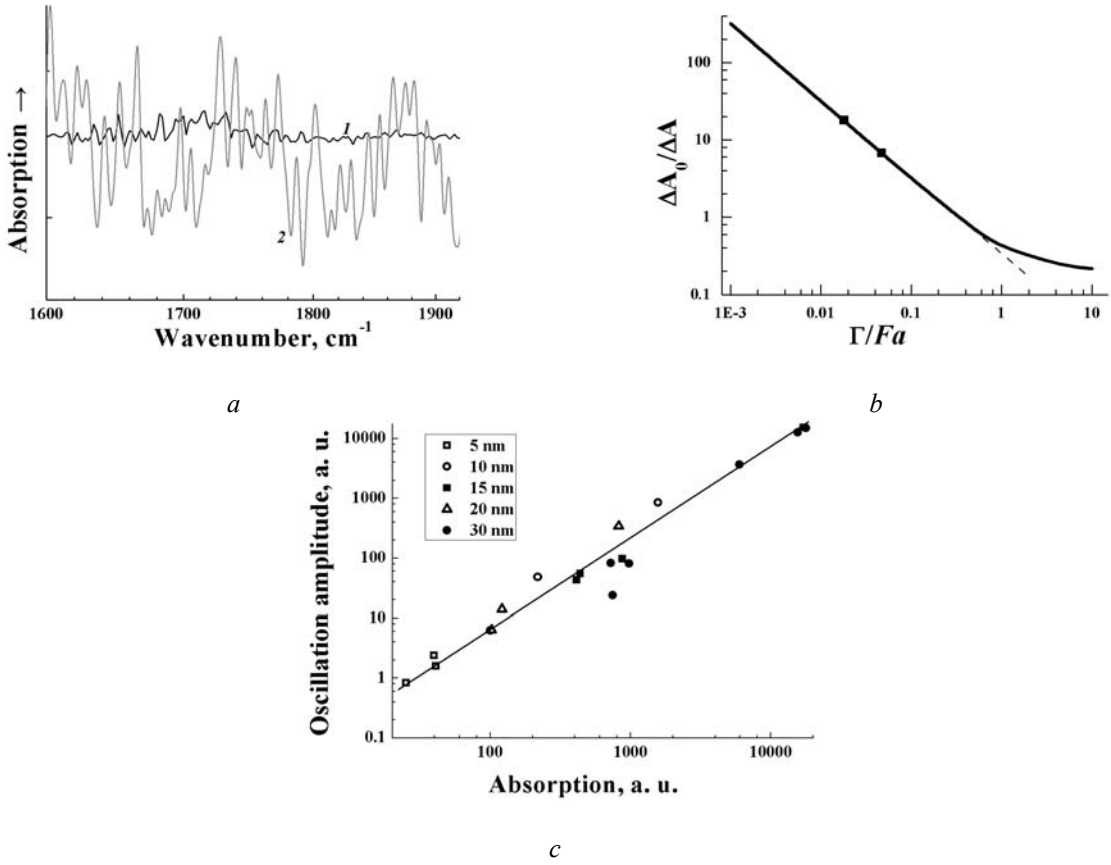

Fig. 4. *a* – a fragment of the IR spectra from Fig. 3 *b* of macroporous silicon after surface cleaning and oxidation to 10 nm thick oxide (*1*) and without surface cleaning and with oxidation to 15 nm thick oxide (*2*), *b* – the results of calculation (curve) of the $\Delta A_0/\Delta A$ dependence on Γ/Fa by Eq. (1). The symbols indicate experimental data from Fig. 3 *b*, *c* – dependencies of oscillation amplitudes on absorption from Fig. 3 *b* for local surface states of oxidized macroporous silicon after preliminary surface cleaning (open symbols) and without surface cleaning (filled symbols)

The calculations of the broadened electro-optical function for the Franz–Keldysh effect were performed in [23]. By analogy with that approach, we determined the effect of broadening on the amplitude of oscillations in IR absorption spectra (ΔA) in the form of convolution of the "non-broadened" oscillation amplitude (ΔA_0) with the Lorentz distribution:

$$\Delta A/\Delta A_0 = \frac{\Gamma}{\pi}\int \frac{d\omega'}{(\omega'-\omega)^2+\Gamma^2} = \arctan(\Delta\omega/\Gamma)/\pi; \qquad (1)$$

where $\Delta\omega = Fa$.

Fig. 4 *b* shows the results of calculation (curve) of the $\Delta A_0/\Delta A$ dependence on Γ/Fa by Eq. (1). The symbols indicate experimental data from Fig. 4 *a* for IR absorption of Si-O-Si

surface states. The values $\Gamma = 0.2 \div 0.5$ cm^{-1} confirm the same period of oscillations (see Fig. 4 *a* and [23]). The obtained values of the broadening parameter Γ correspond to those for surface phonon polaritons measured in thin films of II–VI semiconductors [16].

Let us analyze the dependences of oscillation amplitudes ΔA on absorption A for local surface states of macroporous silicon structures (Fig. 4 *c*). Such dependences for macroporous silicon samples without surface cleaning and with surface oxide of 50–200 nm thick that are linear and correspond to the resonance electron scattering perpendicularly to Si-SiO_2 interface for oxidized macroporous silicon samples [15]. The dependences in Fig. 4 *c* obey the "3/2 law" for the samples after surface cleaning and with surface oxide thicknesses of 10–200 nm. The obtained dependences of oscillation amplitudes ΔA on absorption A correspond to $\Gamma^{-1} \sim \tau \sim E$ or $E^{3/2}$ (where $\tau = \hbar/\Gamma$ is electron scattering lifetime and E is electron energy). Thus, the resonance electron scattering perpendicularly to Si-SiO_2 interface for oxidized macroporous silicon samples without preliminary surface with $\tau_r \sim E$ [15] transforms into ordinary electron scattering by ionized impurities in all directions with law $\tau_I \sim E^{3/2}$ [24] for the samples with surface cleaning and for oxidized macroporous silicon samples without preliminary surface cleaning and oxide thickness less than 30 nm. In the latter case, the counter flow of electrons from the silicon matrix toward the Si-SiO_2 interface grows.

Fig. 5 shows the IR absorption spectra of oxidized macroporous silicon structures without and with a nanolayer of CdS nanoparticles: *a* – without preliminary surface cleaning; *b* – after preliminary surface cleaning.

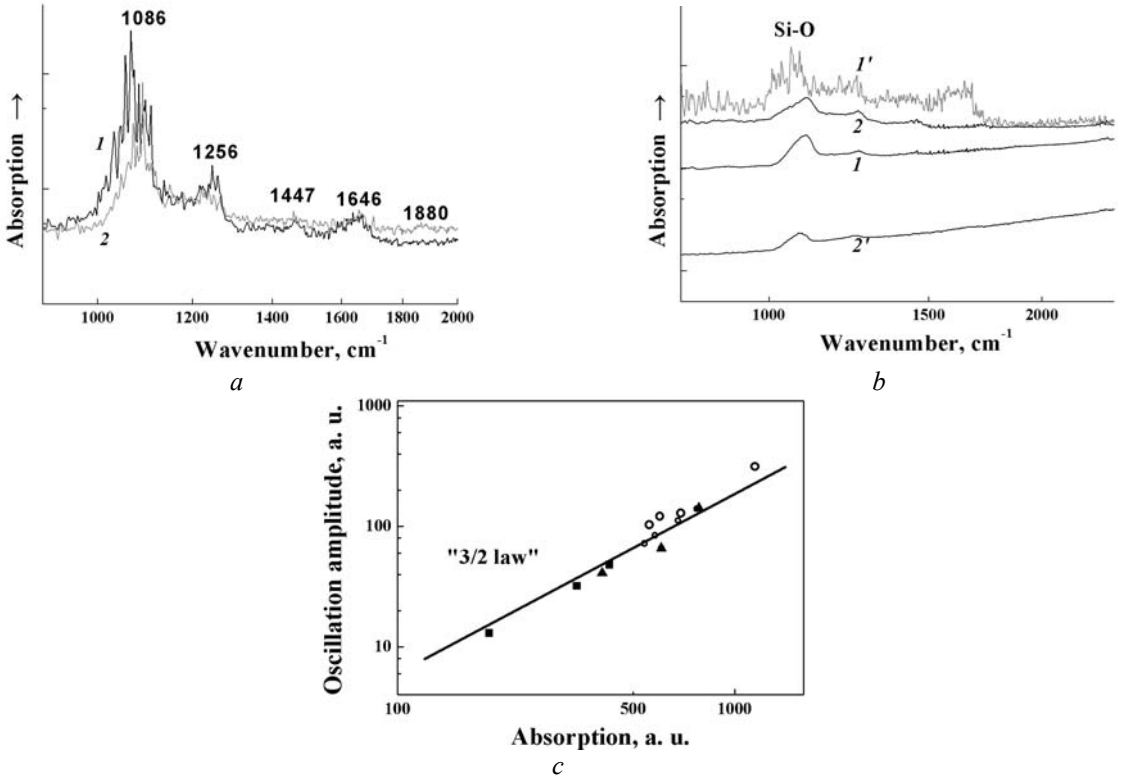

Fig. 5. *a* – IR absorption spectra of oxidized macroporous silicon structures without preliminary surface cleaning and 15 nm thick surface oxide: 1– without and 2 – with a 30 nm thick nanolayer of CdS nanoparticles. *b* – IR absorption spectra of oxidized macroporous silicon structures with preliminary surface cleaning: 1, 1' – 10 nm thick surface oxide; 2, 2' – 20 nm thick surface oxide; 1, 2 – without and 1', 2' – with a 30 nm thick nanolayer of CdS nanoparticles. *c* – dependences of oscillation amplitudes (ΔA) on absorption (A) for macroporous silicon samples with CdS nanocrystals and with the silicon oxide thicknesses 5 nm (■), 10 nm (○) and 20 nm (▲) for local surface states

The IR absorption of oxidized macroporous silicon structures without surface cleaning (Fig. 5*a*) is almost 10 times bigger than that without preliminary surface oxidation (Fig. 5 *b*) due to high concentration of the surface local states. Deposition of a CdS nanolayer increases local electric field at the Si-SiO_2 interface too. The corresponding electric field strength $F = \Delta E/a$ is determined from the energy ΔE between the oscillation maxima and the silicon lattice parameter a [15]. The obtained electric field strength F data vary from $4.5 \cdot 10^4$ to $6.8 \cdot 10^4$ V/cm. The dependences of oscillation amplitudes on absorption for local surface states of oxidized macroporous silicon with a nanolayer of CdS nanoparticles (Fig. 5 *c*) obey the "3/2 law". Thus, the counter flow of electrons from the silicon matrix toward the CdS coating interface grows.

Photoluminescence was measured on oxidized macroporous silicon structures with oxide thickness of 5–20 nm and CdS nanocrystals with thickness of 10–30 nm. Fig. 6 *a* shows the spectral dependence of photoluminescence intensity in macroporous silicon structures with CdS nanocrystals (thickness of 30 nm), the oxide thickness of 5, 10 and 20 nm. The peak of photoluminescence spectra coincides with the corresponding data for aqueous colloidal solution of CdS in polyethyleneimine (2.6-2.7 eV) [1].

The maximal photoluminescence intensity was measured for the structure of macroporous silicon with CdS nanocrystal layer (thickness of 30 nm) and oxide thickness of 10 nm, with the maximal electric field strength $F_S = 6.8 \cdot 10^5$ V/cm at the Si-SiO_2 interface – see Fig. 6 *b*. This indicates a significant decrease in non-radiative recombination of electrons generated on CdS nanocrystals due to the counter flow of electrons from the silicon matrix toward the CdS nanocrystal layer. This process is enhanced by the electron scattering on ionized impurities in all directions for oxidized macroporous silicon samples without preliminary surface cleaning instead of the resonance electron scattering perpendicular to Si-SiO_2 border for oxidized macroporous silicon samples without preliminary surface cleaning.

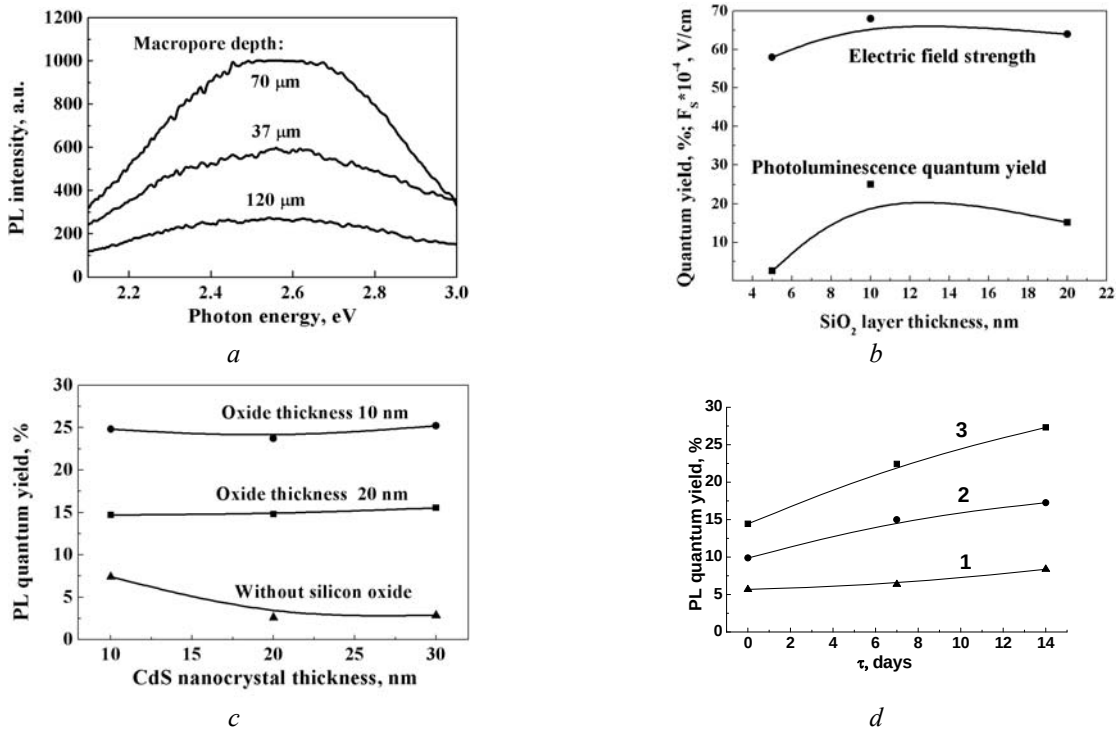

Fig. 6. *a* – Spectral dependence of photoluminescence intensity for the macroporous silicon structures with oxide thickness of 20 nm; *b* – dependence of the photoluminescence quantum yield and electric field strength on the SiO_2 thickness; dependence of the photoluminescence quantum yield on CdS nanocoating thickness (*c*) and on time (*d*)

The photoluminescence quantum yield does not change for macroporous silicon structures with optimal oxide thickness of 10 and 20 nm and decreases for macroporous silicon structures without silicon oxide layer and with thin SiO_2 thickness of 5 nm (Fig. 6 *c*). The photoluminescence spectra and photoluminescence quantum yield were measured 7 and 14 days after the sample preparation. The photoluminescence spectral maximum increases by 4–6 times through 7 days after the sample preparation (Fig. 6 *d*). This indicates a decrease in the rate of non-radiative recombination at the nanocoating as a result of decrease in the concentration of recombination centers in this area of structures. The photoluminescence quantum yield of CdS nanoparticles on the surface of oxidized macroporous silicon with optimum thickness of SiO_2 layer increases by 1.5÷2.3 times and reaches 28 %. With further storage of samples, the spectral range and photoluminescence quantum yield almost did not change. The quantum yield of photoluminescence for such structures increases with time due to evaporation of water molecules from the CdS-polyetheleneimine layer [25]. The obtained value of the photoluminescence quantum yield for investigated nanostructures is comparable with that for CdS quantum dots of 2÷3 nm in size (26–27 %) [1] and after annealing process (29 %) [26].

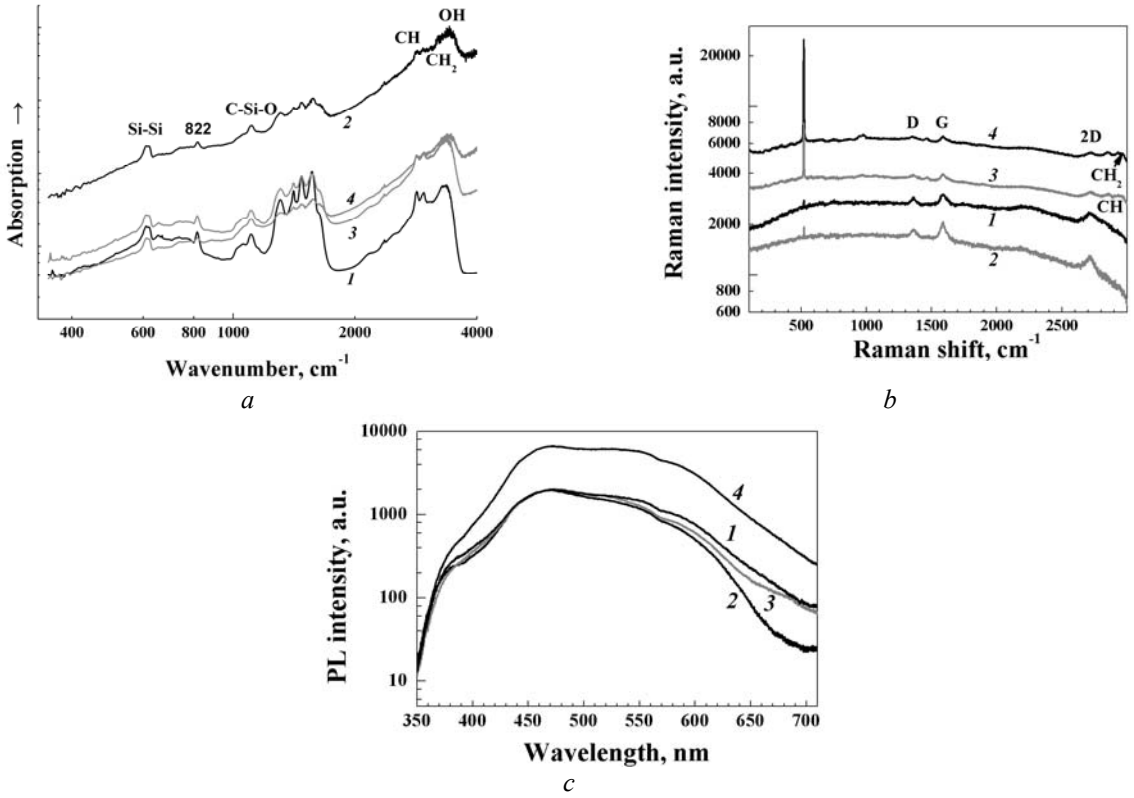

Fig. 7. IR absorption (*a*), Raman (*b*) and photoluminescence (*c*) spectra of macroporous silicon structures with nanocoatings of polyethyleneimine with carbon multiwall nanotubes: *1* – silicon single crystal, *2* – macroporous silicon, *3* – oxidized macroporous silicon, *4* – macroporous silicon with microporous layer

Carbon multiwall nanotubes of 20 nm in diameter (Fig. 2 *b*) were deposited from a colloidal solution of polyethyleneimine in water onto the single crystal silicon, macroporous silicon, oxidized macroporous silicon and macroporous silicon with microporous silicon layer. Fig. 7 *a* shows the IR absorption spectra of macroporous silicon structures with nanocoatings of polyethyleneimine with carbon multiwall nanotubes. IR absorption spectra have the similar peak frequencies of surface states. High IR absorption was measured on macroporous silicon substrate (curve 2). IR absorption for substrates of oxidized

macroporous silicon and macroporous silicon with microporous silicon layer (curves 3, 4) is lower and comparable. Thus, nanocoatings of polyethyleneimine with carbon multiwall nanotubes increase surface depletion [27] and IR absorption of macroporous silicon without nanocoatings and decrease surface accumulation [15, 16] for SiO_2 coatings and microporous silicon layer.

The Raman spectra of macroporous silicon structures with nanocoatings of polyethyleneimine with carbon multiwall nanotubes (Fig. 7 *b*) have carbon-like peaks similar to IR spectra in Fig. 7 *a* (carbon sp^2- and sp^3-hybrid orbitals, CH and CH_2 bonds). The peaks of one-phonon in Si (305 cm^{-1}), two-phonon in Si (514 cm^{-1}), transverse acoustical phonon in Si (TA) and twice carbon sp^3-hybrid orbitals (2D) were measured in Raman spectra only. The maximal Raman shift was measured for macroporous silicon with microporous silicon layer (Fig. 7 *b*, curve 4).

The photoluminescence intensity of polyethyleneimine with carbon multiwall nanotubes is maximal for substrate of macroporous silicon with microporous silicon layer (Fig. 7 *c*, curve 4). The photoluminescence of polymer is determined by exciton generation and electron-hole radiative recombination [28]. The photoluminescence intensity of polyethyleneimine with carbon multiwall nanotubes on macroporous silicon with microporous layer is 5.6 times higher than that of polyethyleneimine with carbon multiwall nanotubes on single crystalline silicon in the photon energy range 2.2–2.7 eV. The microporous layer includes hydrogen atoms [14] and decreases a non-radiative proton recombination on boundary microporous layer and "polymer-nanoparticles" nanocoating.

CONCLUSIONS

Light-emitting coatings of CdS nanocrystals in polyethyleneimine and polyethyleneimine with multiwall carbon nanotubes on silicon substrates have been investigated:

- The maximal photoluminescence intensity was measured for the structure of oxidized macroporous silicon with CdS nanocrystal layer with the maximal electric field intensity at the Si-SiO_2 interface. This indicates a significant decrease of non-radiative recombination of electrons generated on CdS nanocrystals due to the counter flow of electrons from the silicon matrix toward the CdS nanocrystal layer. The photoluminescence quantum yield of CdS nanocrystals on the surface of oxidized macroporous silicon with optimum thickness of SiO_2 layer increases with time up to 28% what is higher than that for CdS quantum dots. With further storage of samples, the spectral range and photoluminescence quantum yield almost do not change.
- The photoluminescence of polyethyleneimine with carbon multiwall nanotubes on macroporous silicon with microporous layer is 3–6 times more intense than that on single crystalline silicon, macroporous silicon and oxidized macroporous silicon. This indicates a non-radiative proton recombination decrease due to hydrogen atoms on boundary silicon matrix with microporous layer and "polymer-nanoparticles" nanocoating.

Owing to the polymer base, the technology makes it possible to increase quantum efficiency of photoluminescence and structure strength as well as to protect the surface from degradation.

ACKNOWLEDGEMENTS

This work was supported by the Project of the China Research Project #2016010010 (Ningbo). We are thankful to Prof. S.Ya. Kuchmii and Dr. A.L. Stroyuk for synthesis of CdS nanocrystals and photoluminescence spectra measurement and to Dr. V.V. Strel'chyk for Raman spectra measurement.

Світловипромінюючі покриття «полімер-наночастинки» на підкладках макропористого кремнію

Л.А. Карачевцева, М.Т. Картель, О.О. Литвиненко, К.П. Конін, В.Ф. Онищенко, Wang Bo

Нінбо технологічний університет, No.55-155 Цуй Бай-роуд, Нінбо, 315016, КНР
Інститут фізики напівпровідників ім. В.Є. Лашкарьова Національної академії наук України
пр. Науки, 41, Київ, 03028, Україна, lakar@isp.kiev.ua
Інститут хімії поверхні ім. О.О. Чуйка Національної академії наук України
вул. Генерала Наумова, 17, Київ, 03164, Україна

Досліджено світловипромінюючі нанопокриття поліетиленіміну з нанокристалами CdS та багатостінними вуглецевими нанотрубками на підкладках макропористого кремнію. Максимальна інтенсивність фотолюмінесценції нанокристалів CdS виміряна при використанні окиснених підкладок макропористого кремнію з максимальною напруженістю електричного поля на межі Si-SiO_2. Квантовий вихід фотолюмінесценції нанокристалів CdS на поверхні окисненого макропористого кремнію збільшується з часом і досягає 28 %. Фотолюмінісценція поліетиленіміну з багатостінними вуглецевими нанотрубками на макропористому кремнії з мікропористим шаром в 3–6 разів більш інтенсивна у порівнянні з підкладками монокристалічного Si, макропористого Si і окисненого макропористого Si внаслідок зниження безвипромінювальної рекомбінації протонів на межі кремнієвої матриці з мікропористим шаром і нанопокриттям.

Ключові слова: *підкладки макропористого кремнію, поліетиленімін, нанокристали CdS, багатошарові вуглецеві нанотрубки*

Светоизлучающие покрытия «полимер-наночастицы» на подложках макропористого кремния

Л.А. Карачевцева, Н.Т. Картель, О.А. Литвиненко, К.П. Конин, В.Ф. Онищенко, Wang Bo

Нинбо технологический университет, No.55-155 Цуй Бай-роуд, Нинбо 315016, КНР
Институт физики полупроводников им. В.Е. Лашкарёва Национальной академии наук Украины
пр. Науки, 41, Киев, 03028, Украина, lakar@isp.kiev.ua
Институт химии поверхности им. А.А. Чуйко Национальной академии наук Украины
ул. Генерала Наумова, 17, Киев, 03164, Украина

Исследованы светоизлучающие нанопокрытия полиэтиленимина с нанокристаллами CdS и многостенными углеродными нанотрубками на подложках макропористого кремния. Максимальная интенсивность фотолюминесценции нанокристаллов CdS измерена при использовании окисленных подложек макропористого кремния с максимальной напряженностью электрического поля на границе раздела Si-SiO_2. Квантовый выход фотолюминесценции нанокристаллов CdS на поверхности окисленного макропористого кремния со временем увеличивается и достигает 28 %. Фотолюминесценция полиэтиленимина с углеродными многостенными нанотрубками на макропористом кремнии с микропористым слоем в 3–6 раз более интенсивна по сравнению с подложками монокристаллического Si, макропористого Si и окисленного макропористого Si вследствие снижения безызлучательной рекомбинации протонов на границе кремниевой матрицы с микропористым слоем и нанопокрытием.

Ключевые слова: *подложки макропористого кремния, полиэтиленимин, нанокристаллы CdS, многослойные углеродные нанотрубки*

REFERENCES

1. Raevskaya A.E., Stroyuk A.L., Kuchmii S.Ya. Optical properties of colloidal CdS nanoparticles stabilized with the sodium polyphosphate and their behaviour under pulse photoexcitation. *Theor. Exp. Chem*. 2003. **39**(3): 158.
2. Chistyakov A.A., Martynov I.L., Mochalov K.E., Oleinikov V.A., Sizova S.V., Ustinovich E.A. Interaction of CdSe/ZnS core–shell semiconductor nanocrystals in solid thin films. *Laser Phys.* 2006. **16**(12): 1625.
3. Trindade T., O'Brien P., Pickett N.L. Nanocrystalline semiconductors: synthesis, properties, and perspectives. *Chem. Mater.* 2001. **13**(11): 3843.
4. Shen Y., Lee Y. Assembly of CdS quantum dots onto mesoscopic TiO_2 films for quantum dot-sensitized solar cell applications. *Nanotechnology.* 2008. **19**(4): 045602.
5. Beato-Lopez J.J., Fernandez-Ponce C., Blanco E., Barrera-Solano C., Ramírez-del-Solar M., Dominguez M. García-Cozar F., Litran R. Preparation and characterization of fluorescent CdS quantum dots used for the direct detection of GST fusion proteins. *Nanomater Nanotechnol*. 2012. **2:** 10.
6. Chestnoy N., Harris T.D., Hull R., Brus L.E. Luminescence and photophysics of cadmium sulfide semiconductor clusters: the nature of the emitting electronic state. *J. Phys. Chem.* 1986. **90**(15): 3393.
7. Jones M., Lo Sh.S., Scholes G.D. Quantitative modeling of the role of surface traps in CdSe/CdS/ZnS nanocrystal photoluminescence decay dynamics. *PNAS*. 2009. **106**(9): 3011.
8. Tomczak N., Jańczewski D., Han M., Vancso G.J. Designer polymer–quantum dot architectures. *Prog. Polym. Sci.* 2009. **34**(5): 393.
9. Kompan M.E., Aksyanov I.G. Near-UV narrow-band luminescence of polyethylene and polytetrafluoroethylene. *Phys. Solid. State*. 2009. **51**(5): 1083.
10. Birner A., Wehrspohn R.B., Gosele U.M., Busch K. Silicon-Based Photonic Crystals. *Adv. Mater*. 2001. **13** (6): 377.
11. Karachevtseva L.A. Two-dimensional photonic crystals as perspective materials of modern nanoelectronics. *Semicond. Phys. Quantum. Electron. Optoelectron.* 2004. **7**(4): 430.
12. Karachevtseva L., Karas' M., Onishchenko V., Sizov F. Surface polaritons in 2D macroporous silicon structures. *Int. J. Nanotechnology*. 2006. **3**(1): 76.
13. Glushko A., Karachevtseva L. Photonic band structure of oxidized macroporous silicon. *Opto-Electron. Rev*. 2006. **14**(3): 201.
14. Cullis A.G., Canham L.T., Calcott P.D.J. The structural and luminescence properties of porous silicon. *J. Appl. Phys*. 1997. **82**(3): 909.
15. Karachevtseva L., Kuchmii S., Lytvynenko O., Sizov F., Stronska O., Stroyuk A. Oscillations of light absorption in 2D macroporous silicon structures with surface nanocoatings. *Appl. Surf. Sci.* 2011. **257**(8): 3331.
16. Karachevtseva L., Goltviansky Yu., Kolesnyk O., Lytvynenko O., Stronska O. Wannier-Stark effect and electron-phonon interaction in macroporous silicon structures with SiO_2 nanocoatings. *Opto-Electron. Rev*. 2014. **22**(4): 201.
17. Nickel N.H., Mei P., Boyce J.B. On the nature of the defect passivation in polycrystalline silicon by hydrogen and oxygen plasma treatments. *IEEE Trans Electron Devices*. 1995. **42**(8): 1559.
18. Lehman V. The Physics of macropore formation in low doped *n*-type silicon. *J. Electrochem. Soc*. 1993, **140(**10): 2836.
19. Karachevtseva L.A., Litvinenko O.A., Malovichko E.A. Stabilization of electrochemical formation of macropores in *n*-Si. *Theor. Exp. Chem*. 1998. **34**(5): 287.
20. Awasthi K., Srivastava A., Srivastava O.N. Synthesis of carbon nanotubes. *J. Nanosci. Nanotechnol*. 2005. **5**(10): 1616.
21. Harrick N.J. *Internal Reflection Spectroscopy*. (New York/London/Sydney: Interscience Publishers, 1967).
22. Seraphin B.O., Bottka N. Band-structure analysis from electro-reflectance studies. *Phys. Rev.* 1966. **145**(2): 628.

23. Enderlein R. The Influence of collisions on the Franz-Keldysh effect. *Phys. Stat. Sol. B.* 1967. **20**(1): 295.
24. Yu P.Y., Cardona M. *Fundamentals of Semiconductors*. (Berlin Heidelberg: Springer-Verlag, 2010).
25. Pokhodenko V.D., Kuchmii S.Ya., Korzhak A.V., Kryukov A.I. Photochemical behavior of nanoparticles of cadmium sulfide in the presence of a reducing agent. *Theor. Exp. Chem.* 1996. **32**(2): 88.
26. Kim J.I., Kim J., Lee J., Jung D., Kim H., Choi H., Lee S., Byun S., Kang S., Park B. Photoluminescence enhancement in CdS quantum dots by thermal annealing. *Nanoscale Res. Lett*. 2012. **7**: 482.
27. Karachevtseva L., Onyshchenko V., Sachenko A. Photocarrier transport in 2D macroporous silicon structures. *Opto-Electron. Rev*. 2010. **18**(4): 394.
28. Thostensona E.T., Renb Z., Chou T. Advances in the science and technology of carbon nanotubes and their composites: a review. *Compos. Sci. Technol*. 2001. **61**(13): 1899.

Received 20.09.2016, accepted 06.02.2017